Method of control and schematic design of a machine irrigation pumping station using a working electrical shaft system

Olimjon Toirov[1], Salikhdjan Khalikov[1], Fozil Sharopov[2,a)], Hao Chen[3], Dilnoza Jumaeva[4]

[1]*Tashkent State Technical University, Tashkent, Uzbekistan*
[2] *Institute of Energy Problems of the Academy of Sciences of the Republic of Uzbekistan, Tashkent, Uzbekistan*
[3]*China University of Mining and Technology, China*
[4]*Institute of General and Inorganic Chemistry of the Academy of Sciences of Uzbekistan, Tashkent, Uzbekistan*

[a)] *Corresponding author: sharopovfozilqobilovich@gmail.com*

Abstract. The article presents a control method and a schematic design of a pumping station configured with two pump units connected to a single common pipeline through the application of a common working electrical shaft (WES), as well as a working electrical shaft system with parametric control. Mathematical expressions for the torque of the induction motors of the working electrical shaft with parametric control are derived by substituting current expressions formulated on the basis of the equivalent circuit, and torque characteristics are constructed taking into account the thyristor firing angle. Experimental investigations of the working electrical shaft with thyristor commutators were carried out on a laboratory test bench.

INTRODUCTION

At present, great importance worldwide is attached to improving technical and technological solutions that ensure stable and safe operation while simultaneously reducing the electrical energy consumption of pumping stations (PS) used for water extraction. Currently, "…37.2% of global energy consumption is attributed to the manufacturing industry, of which 20% is consumed by pumping stations; measures to increase their reliability and safety through technical modifications, as well as to reduce energy consumption, are being considered" [1–3]. A significant place in the economic complex of the Republic of Uzbekistan is occupied by machine irrigation, implemented through water–lifting pumping stations. The efficiency of operation of pumping units in machine water–lifting systems, and consequently of pumping stations, is largely determined by the quality of regulation and control of technological water–supply processes with the implementation of water– and energy–saving technologies. Therefore, the control of pumping stations aimed at achieving energy– and resource–saving operating modes through the use of automated electric drive systems, while ensuring compliance with the requirements of the water–supply technological process, is an urgent problem. Its solution makes it possible to save significant amounts of electrical energy and irrigation water [4–6]. In existing irrigation pumping stations of the Republic of Uzbekistan, there are configurations of pumping units in which two or more pump units are connected to a single common pipeline. In such an operating mode, if one of the pumps operating in parallel has a higher flow rate and head, the pump with a lower flow rate and head will be "suppressed" by the other pump, which leads to the occurrence of system vibrations and possible damage to the common pipeline. To prevent these events, the pump flow rates are first equalized, and only after that are they connected to the common pipeline [7–10]. In existing pumping stations, flow equalization is carried out using valves installed on the discharge pipeline of each pumping unit. With this method of equalization, synchronized rotation is ensured with deviations in water flow rate and head [11–13]. Taking this into account, the authors have developed a control method for a pumping station and a device for its implementation [14-15]. To implement the method using a conventional working electrical shaft (WES) (with RT1 and RT2 not connected to the rotor circuits), after connecting induction motors IM1 and IM2 with different rotational speeds ($n_1 \neq n_2$), i.e., pump units PU1 and PU2 with different water flow rates ($Q_1 \neq Q_2$), an equalizing current I_eq flows through the rotor circuits. Due to this current, the rotational speeds of the motors ($n_1 \neq n_2$) and the water flow rates ($Q_1 \neq Q_2$) are equalized. After that, from the output of the comparison block CB, the signal $Q\_\Sigma = Q_1 + Q_2$ is supplied to the input of the water flow setpoint unit WFS and is compared with the specified water flow rate Q_set of the pumping station. If $Q\_\Sigma \neq$ Q_set, the signal taken from the summator of the WFS is fed to the input of the control unit CU of the frequency converter FC and smoothly changes the rotational speeds of induction motors IM1 and IM2, thereby changing the flow rates of the controlled pumps P1 and P2 until the water flow rate pumped by the station corresponds to its supply schedule (Figure 1). The working electrical shaft (WES) differs from other systems by its simplicity and does not require high operating costs. Theoretical and experimental studies of the working electrical shaft system with an extended operating range based on parametric control using series–parallel connected thyristors connected to the three phases of the rotor circuit have been carried out [16]. Expressions for rotor currents, voltages, and torques have been obtained, and torque characteristics revealing the properties of the system under consideration have been constructed. Let us consider the operating principle of this WES system. The rotor windings of motors IM1 and IM2 are represented as separate sections moving relative to the stator field, as described in [17].

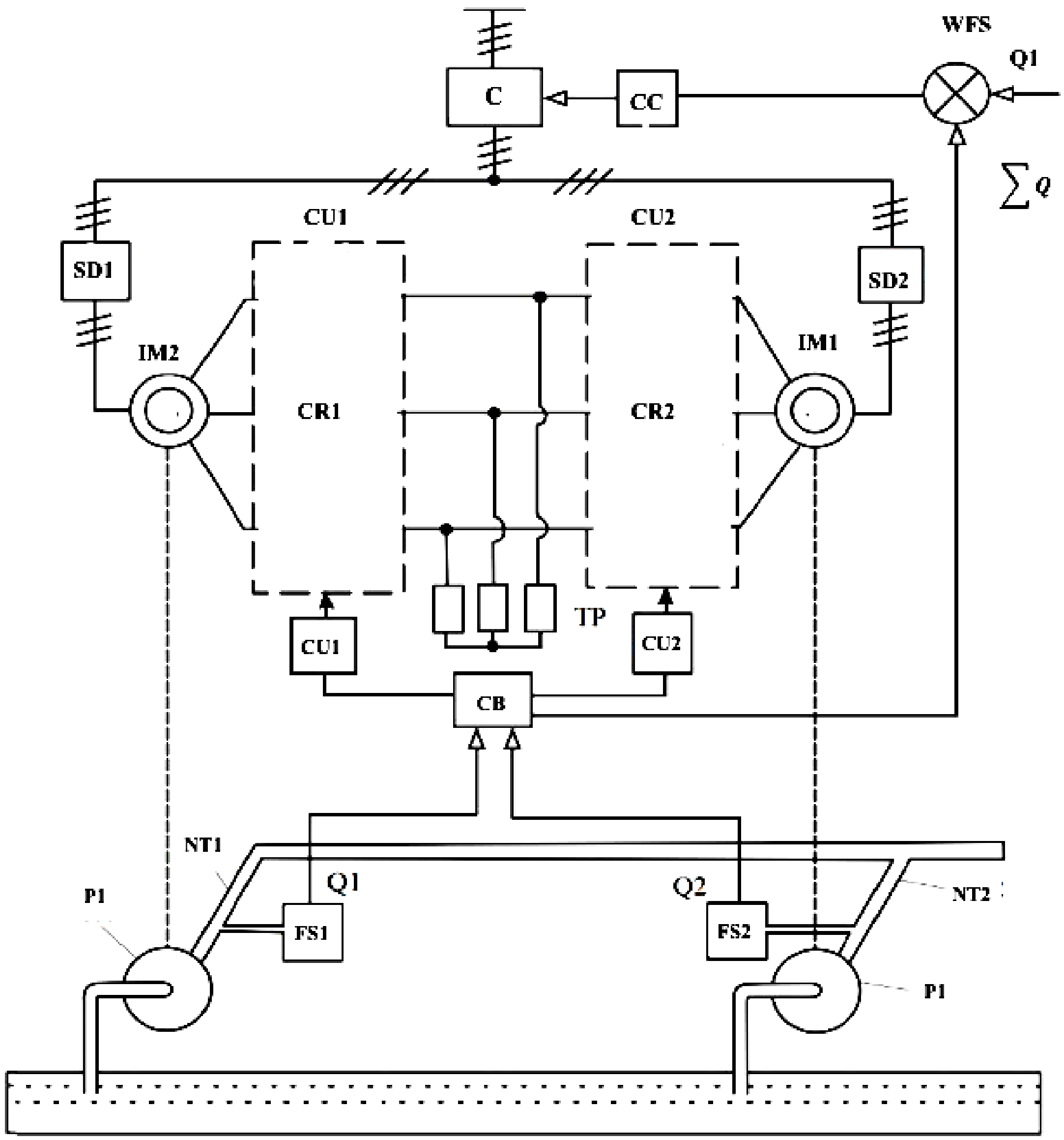

FIGURE 1. Schematic diagram of the pumping station control method using a working electrical shaft (WES) with parametric control.

P1, P2 – pumps; DP1, DP2 – discharge pipelines; FS1, FS2 – water flow sensors; IM1, IM2 – induction motors; CU1, CU2 – control units; CR1, CR2 – current regulators; CB – comparison block; SD1, SD2 – starting devices; FC – frequency converter; CC – frequency converter control unit; WFS – water flow setpoint unit.

When a difference in static torques occurs ($M_{S1} \neq M_{S2}$), the rotor of the more heavily loaded motor lags behind the rotor of the less heavily loaded motor. As a result, a rotor position mismatch angle θ and an equalizing torque arise. The equalizing torque maintains synchronous rotation by unloading the more heavily loaded motor and loading the less heavily loaded motor. However, when the difference in static torques is large, the equalizing torque in a conventional WES scheme cannot maintain coordinated rotation of the motors. As a result, the motors lose synchronous operation, and the rotor of the less heavily loaded motor accelerates. The schematic diagram of the proposed WES system with series–parallel connected thyristor commutators connected to the three phases of the rotor circuits is shown in Fig. 2. In this scheme, series–parallel connected thyristors T1 and T2, T3 and T4, T5 and T6, which are part of current regulator CR1, are connected to the three phases of the rotor circuit of induction motor IM1 between the rotor winding and the common resistance R. Similarly, thyristors T7 and T8, T9 and T10, T11 and T12, which are part of current regulator CR2, are connected to the three phases of the rotor circuit of induction motor IM2 between the rotor winding and the common resistance R [18-20].

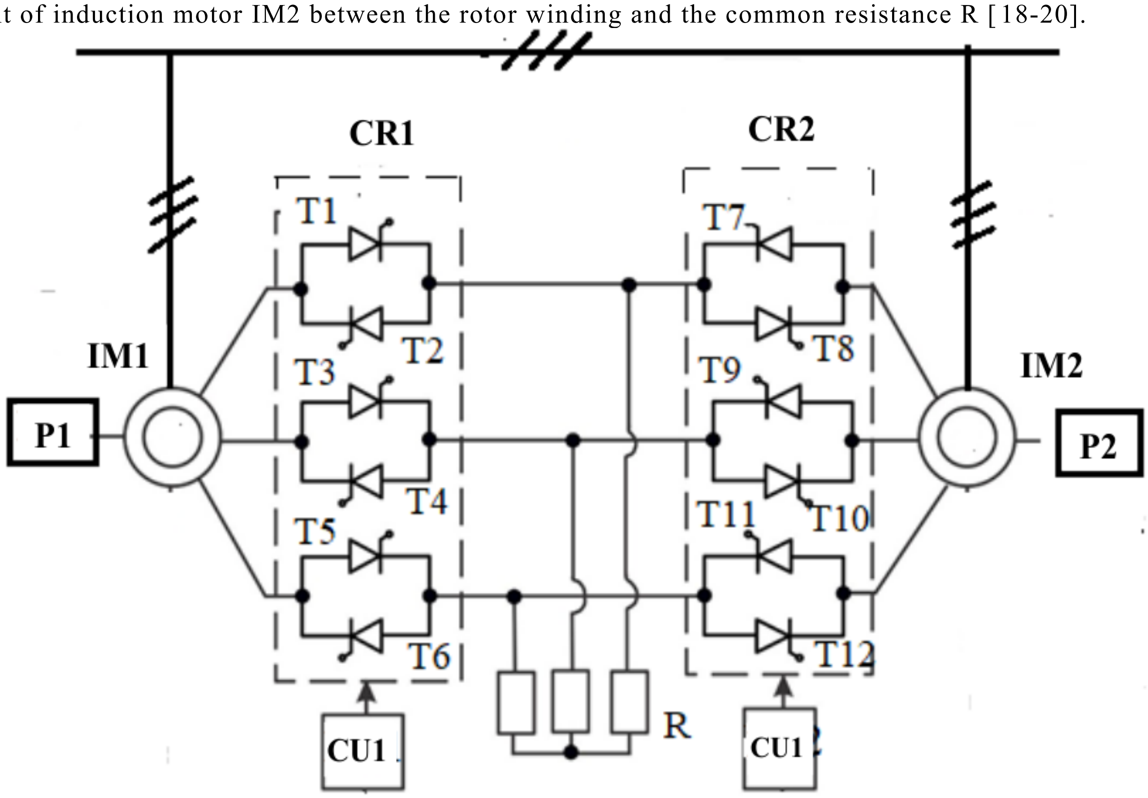

FIGURE 2. Schematic diagram of the working electrical shaft (WES) with parametric control when series–parallel connected thyristors are connected to the three phases of the rotor circuits of an induction motor.

In addition, this configuration of the valves makes it possible to perform synchronization on the fly, that is, to switch on motors IM1 and IM2 with different shaft loads ($M_{s1} \neq M_{s2}$). Let motors IM1 and IM2 rotate separately at different rotational speeds. As is known, at the moment of switching on, under the action of the asynchronous electromagnetic torque, the rotor of the motor with the lower load accelerates, and its rotational speed exceeds that of the more heavily loaded motor. As a result, the motors of the system do not synchronize and accelerate asynchronously [21-23]. In this case, the braking torque created by introducing the thyristor valves also prevents the acceleration of the rotor of the less heavily loaded motor, thereby ensuring a favorable relative position of the rotors.

EXPERIMENTAL RESEERARCH

Taking into account the adopted assumptions, we will develop the equivalent circuit for the considered parametric-control REW system (Fig. 3). The following assumptions are made here:

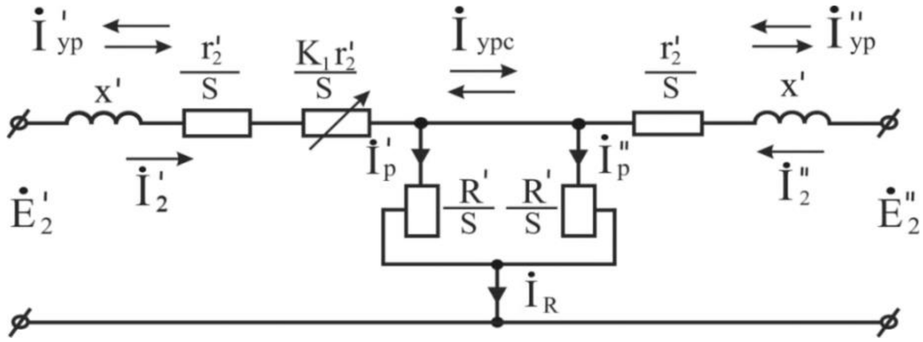

FIGURE 3. Equivalent circuit of the working electrical shaft (WES) with parametric control when series–parallel connected thyristors are connected to the three phases of the rotor circuits of an induction motor.

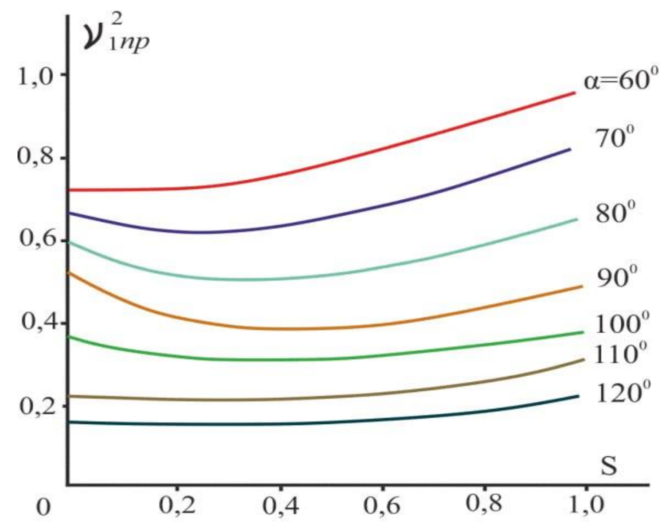

FIGURE 4. Dependencies $\nu_1^2 = f(s)$

Using the dependencies $\nu_1^2 = f(\alpha, \varphi)$ и φ = f(s) – a family of curves $\nu_1^2 = f(s)\nu_1^2 = \ f(s)$ was obtained for AK–61/4 type motors, taking into account the construction method presented in [24]. These curves are shown in Fig. 4. This dependence will be used as coefficients in the equivalent circuit (Fig. 3), and the corresponding dependencies will be applied as coefficients $К_1 = \nu_1^2 = f(s)$.

The torque expressions for motors IM1 and IM2 in the considered WES system are determined by substituting the current expressions derived on the basis of the equivalent circuit shown in Fig. 3. The torque equations for the case Mc1<Mc2 take the following form:

$$M_1 = 2M_{к}x\left\{\frac{\left[\left(\frac{r_2' + 2R'}{S}\right)\frac{r_2'}{S}\left(\frac{r_2'(1+K_1)}{S}\right) + x^2\right] + \frac{r_2' \cdot K_1}{S}\left(\frac{r_2' + R'}{S}\right)\left(\frac{r_2'(1+K_1)}{S}\right) +}{F_{зн}}\right.$$

$$\frac{+\left[\left(\frac{r_2' + 2R'}{S}\right)\left(\frac{r_2'(1+K_1)}{S}\right) - \left(\frac{r_2' \cdot K_1 \cdot R_1}{S^2}\right) - X^2\right]\left[\left(\frac{R' - r_2' \cdot K_1}{S}\right) - \frac{R'}{S}\cos\theta\right]}{1}$$

$$-\frac{\frac{R'}{S}x\left[\left(\frac{r_2'}{S}+\frac{r_2'+2R'}{S}\right)+\frac{r_2'\cdot K_1}{S}\right]sin\theta}{1}\Bigg\} \quad (1)$$

where the denominator values F_{3H}:

$$F_{зн}=\left[\ \left(\frac{r_2'+2R'}{S}\right)^2+x^2\right]\left[\left(\frac{r_2'(1+K_1}{S}\right)^2+x^2\right]-2\left(\frac{r_2'\cdot K_1\cdot R'}{S^2}\right)\left[\left(\frac{r_2+2R}{S}\right)\cdot\left(\frac{r_2'(1+K_1}{S}\right)-x^2\right]+\left(\frac{r_2'\cdot K_1\cdot R}{S^2}\right)^2$$

$$M_2=M_к\left[\frac{1-cos\theta+\frac{S}{S_k}sin\theta}{\frac{S}{S_k}+\frac{S_k}{S}}+\frac{1+cos\theta+\frac{S}{S_k'}sin\theta}{\frac{S}{S_k'}+\frac{S_k'}{S}}\right] \quad (2)$$

where:

$x=x_1+x_2';\ S_k'=[(r_2'+2R')/r_2']S_k$

M_1, M_2 – the electromagnetic torques of induction motors IM1and IM2;
$M_К$ – critical torque of induction motors IM1 and IM2;
S– slip of induction motors IM1 and IM2;
S_K – critical slip of induction motors IM1 and IM2;
Θ– rotor position mismatch (displacement) angle;
x_1–inductive reactance of the stator winding of the induction motor.
x_2' – rotor winding inductive reactance referred to the stator;
R' – total resistance referred to the stator.

RESEARCH RESULTS

The variation of the normalized torques M_1/M_K and M_2/M_K or the WES system with thyristor commutators connected to the three phases of the rotor circuit of the less heavily loaded induction motor IM1 (IM1<IM2) at different values of the thyristor firing angle α, is shown in Fig. 5.

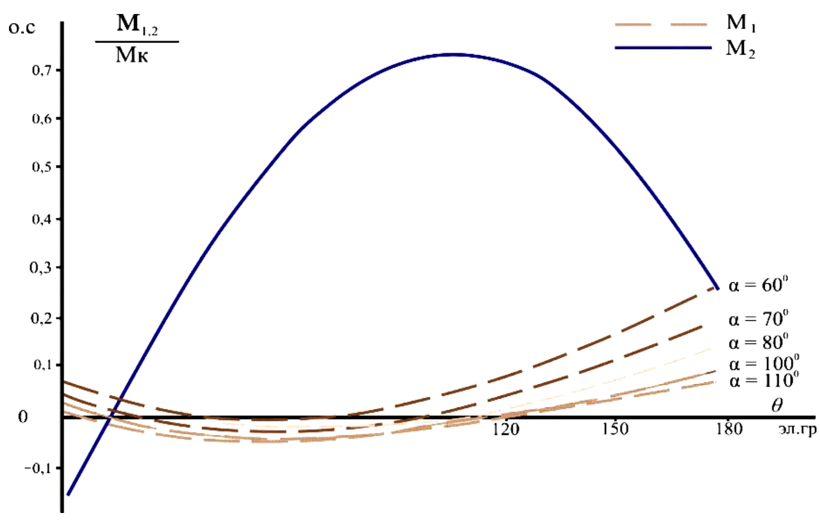

FIGURE 5. The dependences $M_{1,2}/M_K=f(\theta)$ РЭВ for the WES with thyristor commutators in the three phases of the rotor circuit of the less heavily loaded motor, for the case Mc1< Mc2 are presented.

The properties of the conventional WES and the parametric–control WES (WES–PC) were investigated on an experimental setup consisting of two induction motors of the AK–61/4 type.

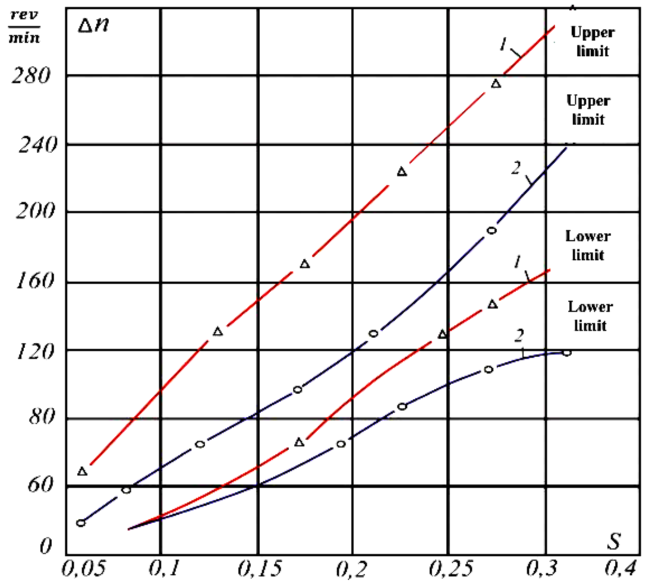

FIDURE 6. Experimental characteristics Δn =f (s).

1 – WES system with parametric control (WES–PC);
2 – conventional WES.

To determine the operating capability of the considered WES systems with thyristor commutators, their operating range was defined. For this purpose, experimental data were obtained, on the basis of which the dependences Δn=(s) (рис.6), were constructed (Fig. 6), where curve 2 corresponds to the conventional WES, and curve 1 corresponds to the WES with thyristor commutators. Here, $\Delta n$is the difference in rotational speeds of the induction motors recorded during their separate rotation after entering synchronism (lower boundary) and upon loss of synchronism (upper boundary); s – is the slip recorded at the moment of entering synchronism and just before loss of synchronism.

CONCLUSIONS

1. The application of the proposed control method and device eliminates the “suppression” of a pump unit with lower flow rate and head by a pump unit with higher flow rate and head, as well as the occurrence of system vibrations and pump shutdowns.
2. The absence of valves, which frequently fail and require repair, leads to a reduction in repair time. As a result, downtime and maintenance time of the pump units are reduced, thereby increasing the reliability of the pumping station.
3. To confirm the validity of the analytical conclusions and the correctness of the proposed calculation methods, experimental studies were carried out on a laboratory setup consisting of two induction motors with identical parameters.
4. It was experimentally established that, when using the WES system with parametric control, the operating range increases by 1.32–1.5 times compared to the conventional WES system.

REFERENCES

1. O. Toirov, A. Khalbutaeva, Z. Toirov. Calculation of the magnetic flux with considering nonlinearities of saturation of the magnetic circuit of synchronous motors, // 3rd International Scientific and Technical Conference on Actual Issues of Power Supply Systems, ICAIPSS 040022, (2023). https://doi.org/10.1063/5.0218821

2. S. Khalikov, Research and Evaluation of the Reliability Indicators of Pumping Units for Mechanical Irrigation of the Pumping Station “Kyzyl-Tepa” Power Technology and Engineering, 57 (5), pp. 690 - 696, (2024). https://doi.org/10.1007/s10749-024-01720-2
3. V. Tsypkina, V. Ivanova, D. Isamukhamedov, M. Kozlitin, Z. Toirov. Overview of Modern Materials Used for the Production of Optical Fiber for Fiber Optic Cables AIP Conference Proceedings, 3331 (1), 050029 (2025). https://doi.org/10.1063/5.0305669
4. O. Toirov, M. Taniev, B. Safarov, Z. Toirov. Simulation model of an asynchronous generator integrated with a power supply system at different wind speeds AIP Conference Proceedings, 3331 (1), 060025, (2025). https://doi.org/10.1063/5.0305672
5. T. Sadullaev, U. Hoshimov, S. Urokov, A. Naimov, J. Khudoyorov, Z. Toirov. Development of an integrated method for rating electrical energy consumption during the drilling process, // AIP Conference Proceedings, 3331 (1), 050028, (2025). https://doi.org/10.1063/5.0305668
6. O. Toirov, W. Yu. Non-Intrusive Load Monitoring Based on Image Load Signatures and Continual Learning // Proceedings of 2025 2nd International Conference on Digital Society and Artificial Intelligence, (2025) https://doi.org/10.10.1145/3748825.3748963
7. N. Avezova, O. Toirov, A. Usmanov. Review of Modern Approaches in the Development of Hybrid Biogas Systems // Applied Solar Energy, 60 (6), (2024) https://doi.org/10.3103/S0003701X25600845
8. O. Filina, A. Khusnutdinov, O. Toirov, Kh. Vakhitov, A. Abdyllina, Investigation the conditions of existence and disturbances of brush-collector contact // E3S Web Conf. 563, 01009, (2024). https://doi.org/10.1051/e3sconf/202456301009
9. D. Jumaeva, O. Toirov, B. Numonov, N. Raxmatullaeva, M. Shamuratova. Obtaining of highly energy-efficient activated carbons based on wood, // E3S Web of Conferences 410, 01018, (2023). https://doi.org/10.1051/e3sconf/202341001018
10. D. Jumaeva, O. Toirov, U. Raximov, O. Ergashev, A. Abdyrakhimov. Basic thermodynamic description of adsorption of polar and nonpolar molecules on AOGW, // E3S Web of Conferences 425, 04003 (2023) https://doi.org/10.1051/e3sconf/202343401020
11. O. Toirov, M. Taniev, M. Hamdamov, A. Sotiboldiev, Power Losses Of Asynchronous Generators Based On Renewable Energy Sources E3S Web of Conferences, 434, 01020, (2023) https://doi.org/10.1051/e3sconf/202343401020
12. O. Toirov, S. Khalikov, Sodikjon Khalikov, F. Sharopov, Studies of reliability indicators of pumping units of machine irrigation on the example of the “Namangan” pumping station, // E3S Web of Conferences 410, 05015, (2023). https://doi.org/10.1051/e3sconf/202341005015
13. D. Bystrov, S. Giyasov, M. Taniev, S. Urokov. Role of Reengineering in Training of Specialists // ACM International Conference Proceeding Series (2020) https://doi.org/10.1145/3386723.3387868
14. O. Toirov, V. Ivanova, V. Tsypkina, D. Jumaeva, D. Abdullaeva, Improvement of the multifilament wire lager for cable production, // E3S Web of Conferences 411, 01041 (2023), https://doi.org/10.1051/e3sconf/202341101041
15. T. Kamalov, U. Mirkhonov, S. Urokov, D. Jumaeva, The mathematical model and a block diagram of a synchronous motor compressor unit with a system of automatic control of the excitation // E3S Web of Conferences, 288, 01083, (2021), https://doi.org/10.1051/e3sconf/202128801083
16. O. Toirov, S. Urokov, U. Mirkhonov, H. Afrisal, D. Jumaeva, Experimental study of the control of operating modes of a plate feeder based on a frequency-controlled electric drive, // E3S Web of Conferences, SUSE-2021, 288, 01086 (2021). https://doi.org/10.1051/e3sconf/202128801086
17. S. Khalikov, Diagnostics of pumping units of pumping station of machine water lifting, // E3S Web of Conferences 365, 04013, (2023). https://doi.org/10.1051/e3sconf/202336504013
18. D. Bystrov, M. Gulzoda, Y. Dilfuza, Fuzzy Systems for Computational Linguistics and Natural Language (2020) // ACM International Conference Proceeding Series, https://doi.org/10.1145/3386723.3387873
19. O. Toirov, I. Khujaev, J. Jumayev, M. Hamdamov, Modeling of vertical axis wind turbine using Ansys Fluent package program, // E3S Web of Conferences 401, 04040 (2023). https://doi.org/10.1051/e3sconf/202340104040
20. O. Toirov, S. Abdi Yonis, Z. Yusupov, A. Habbal, Control Approach Of A Grid Connected Dfig Based Wind Turbine Using Mppt And Pi Controller, // Advances in Electrical and Electronic Engineering, 21, 3, (2023). https://doi.org/10.15598/aeee.v21i3.5149
21. D. Jumaeva, A. Abdurakhimov, Kh. Abdurakhimov, N. Rakhmatullaeva, O. Toirov, Energy of adsorption of an adsorbent in solving environmental problems, // E3S Web of Conferences, SUSE-2021, 288, 01082 (2021). https://doi.org/10.1051/e3sconf/202128801082

22. O. Toirov, M. Khalikova, D. Jumaeva, S. Kakharov, (2023) Development of a mathematical model of a frequency-controlled electromagnetic vibration motor taking into account the nonlinear dependences of the characteristics of the elements, // E3S Web of Conferences 401, 05089, (2023). https://doi.org/10.1051/e3sconf/202340105089
23. O. Toirov, S. Khalikov. Analysis of the safety of pumping units of pumping stations of machine water lifting in the function of reliability indicators, // E3S Web of Conferences 365, 04010 (2023), https://doi.org/10.1051/e3sconf/202336504010
24. Sh. Azimov, Z. Najmitdinov, M. Sharipov, Z. Toirov. Improvement of the cooling system of reactive power compensating devices used in railway power supply // E3S Web of Conferences, 497, 01015, (2024). https://doi.org/10.1051/e3sconf/202449701015